IEEE Photonics Journal
An IEEE Photonics Society Publication

Blind Frequency Offset Estimation Based on Phase Rotation For Coherent Transceiver

Volume 12, Number 2, April 2020

Qingzhao Tan
Aiying Yang
Peng Guo
Zhao Zhao

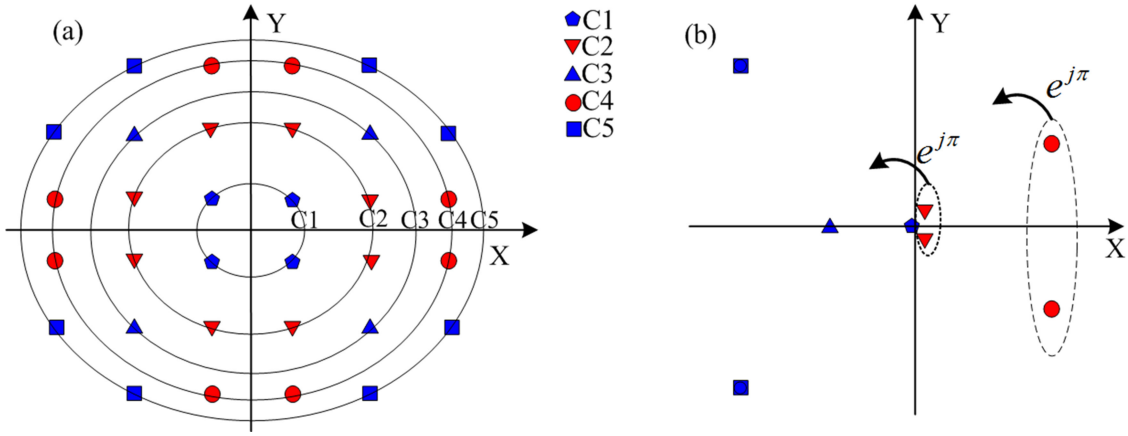

DOI: 10.1109/JPHOT.2020.2983086

Blind Frequency Offset Estimation Based on Phase Rotation For Coherent Transceiver

Qingzhao Tan, Aiying Yang, Peng Guo, and Zhao Zhao

Key Laboratory of Photonics Information Technology, Ministry of Industry and Information Technology, School of Optics and Photonics, Beijing Institute of Technology, Beijing 100086, China

DOI:10.1109/JPHOT.2020.2983086

Manuscript received December 25, 2019; revised March 11, 2020; accepted March 21, 2020. Date of publication March 30, 2020; date of current version April 16, 2020. This work was financially supported in part by the National Natural Science Foundation of China under Grant 61427813, in part by the Open Fund of IPOC (BUPT) under Grant IPOC2018B003, and in part by the State Key Laboratory of Advanced Optical Communication Systems and Networks China. Corresponding authors: Aiying Yang; Peng Guo (e-mail: yangaiying@bit.edu.cn; guopeng0304@bit.edu.cn).

Abstract: Conventional fast Fourier transform based frequency offset estimation (FFT-FOE) algorithm is suitable for QPSK and 8/16/64QAM signals. However, due to the non-rectangular distribution of constellation points, the conventional FFT-FOE is not suitable for 32-QAM signal. In this paper, we report a factor γ which can indicate whether the FFT-FOE algorithm can be used for frequency offset estimation for different modulation formats. The FFT-FOE algorithm is hard to apply for frequency offset estimation if the value of γ is low. Fortunately, the value of γ can be increased by digital amplification and phase rotation. Based on the digital amplification and phase rotation, a modified FFT-FOE algorithm is proposed and can realize the frequency offset estimation of 32-QAM signal with only 512 symbols. The bit error ratio (BER) of a 28 Gbaud 32-QAM signal is lower than the soft-decision forward-error correction (SD-FEC) limit with the optical signal-to-noise ratio (OSNR) of 22 dB. The proposed method has better robustness to phase noise. If BER at SD-FEC limit is considered for 28Gbaud 32-QAM signal, the required OSNR is relaxed by 2 dB when the laser linewidth is greater than 5 MHz. This will make sense when the wide-linewidth laser is used in short reach optical communication system. The experimental results from 10 Gbaud 32-QAM system with 300 km fiber transmission indicate that the proposed method can be applied when OSNR is greater than 14 dB. The results demonstrate that the proposed frequency offset estimation scheme is also suitable for QPSK and 8/16/64QAM signals. Thus, the proposed algorithm can perform blind frequency offset estimation for a coherent transceiver.

Index Terms: Frequency offset estimation, amplification and phase rotation, fast Fourier transform.

1. Introduction

With the development of the internet and the increasing demand for IP traffic, optical networks have gradually evolved from fixed architectures to flexible architectures, which can increase spectral efficiency by modulation format switching [1]–[3]. For such coherent transceiver, the digital signal processing (DSP) algorithms at the receiver-side should be reconfigured under the condition of modulation format switching. In [4]–[6], the frequency offset estimation is considered to be

performed after modulation format identification. Therefore, a new frequency offset estimation algorithm that can be applied before modulation format identification for coherent transceiver is meaningful.

Up to now, non data-aided [7], [8] frequency offset estimation can be divided into two categories. The first type relies on differential phase [9]–[12]. The differential frequency offset estimation (diff-FOE) is designed for M-ary phase shift keying (M-PSK) format, which is also suitable for 16 quadrature amplitude modulation (QAM) using quadrature phase shift keying (QPSK) partitioning [10]. In order to apply for higher order QAM signal, diff-FOE based on constellation rotation was proposed [11], [12]. However, the proposed method above is not transparent to different modulation formats. The other kind of frequency offset estimation is based on fast Fourier transform [13]–[16]. Since the fourth-order constellations of QPSK and 8/16/64QAM signals are non-circular, conventional fast Fourier transform based frequency offset estimation (FFT-FOE) can be used for identifying respective frequency offsets. Meanwhile, it is known that FFT has high complexity which is related to FFT size. Considering the computation complexity, the FFT size must choose a reasonable length during the real-time implementation. In refs. [13], [15], the FFT size is chosen as 512 for QPSK and 8/16/64QAM signals using conventional FFT-FOE. However, due to the non-rectangular distribution of constellation points, the conventional FFT-FOE cannot be applied to the 32-QAM signal with 512 symbols unless there are huge number of symbols. To solve this problem, a FFT-FOE technique by selecting and digitally amplifying the inner QPSK ring of 32-QAM signal was reported in [16]. However, the authors think that the constellation points on the diagonal line with slope equal to $+1$ or -1 have most important contributions to search the intensity peak in spectrum and ignore the residual constellation points.

In this paper, we propose a digital amplification and phase rotation based FFT-FOE algorithm for coherent transceiver, which is transparent to QPSK and 8/16/32/64QAM signals. The factor γ is proposed to indicate whether the FFT-FOE algorithm can be used for frequency offset estimation. The same as conventional FFT-FOE, the phase rotation based FFT-FOE algorithm has the advantages of wide frequency offset estimation range of [$-$symbol rate/8, $+$symbol rate/8] and robustness to amplified spontaneous emission (ASE) noise and phase noise. The results show that the bit error ratio (BER) of a 28 Gbaud 32-QAM signal is lower than the soft-decision forward-error correction (SD-FEC) limit with the optical signal-to-noise ratio (OSNR) of 22 dB. The experimental results from 10 Gbaud 32-QAM system with 300 km fiber transmission indicate that the proposed method can be applied when OSNR is greater than 14 dB.

2. Principle of Phase Rotation Based Frequency Offset Estimation

2.1 Conventional Frequency Offset Estimation Based on FFT

At the coherent receiver side, the received signal after analog-to-digital conversion (ADC), chromatic dispersion (CD) compensation, clock recovery and polarization mode dispersion (PMD) compensation, the n^{th} received symbol can be expressed as:

$$S_n = m_n e^{j(2\pi n \Delta f T_s + \theta_n)}, \quad 1 \le n \le N \tag{1}$$

where m_n is the n^{th} data symbol, Δf is the frequency offset, T_S is the symbol duration, N is the number of symbols, and θ_n is the phase noise induced by laser linewidth. For the conventional FFT-FOE, the frequency offset Δf can be obtained based on the maximization of the periodogram S_n^4 as expressed below [13]:

$$\Delta f = \frac{1}{4} \arg \max_{|\Delta \hat{f}| < 1/2T_s} \left| \sum_{n=0}^{N-1} S_n^4 e^{-j2\pi n \Delta \hat{f} T_s} \right| \tag{2}$$

where $\arg\max_{|\Delta \hat{f}| < 1/2T_s}(.)$ represents the operation of searching $\Delta \hat{f}$ within the range of [$-$symbol rate/2, $+$symbol rate/2], when the function (.) value is maximized. The frequency offset can be easily estimated if the spectrum intensity peak of S_n^4 determined by $|\sum_{n=0}^{N-1} m_n^4|$ is high. Fig. 1 shows

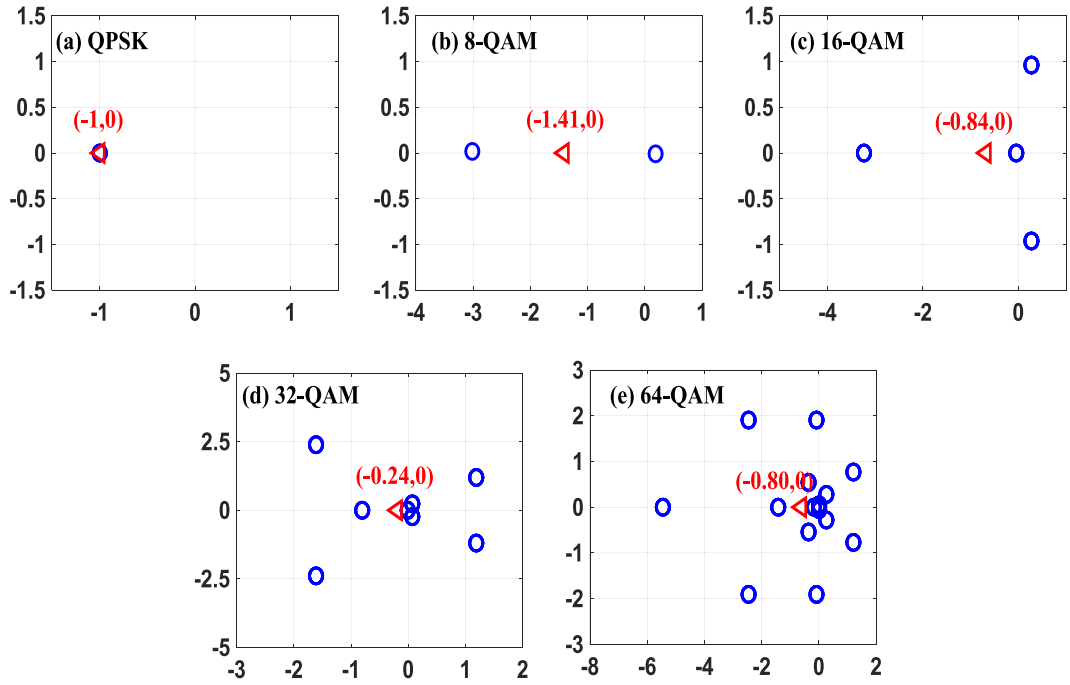

Fig. 1. The constellation points after the 4th power operation (blue point) and its centroid (red point) of (a) QPSK, (b) 8-QAM, (c) 16-QAM, (d) 32-QAM, and (e) 64-QAM.

the constellation points after the 4th power operation (m_n^4) and its centroid ($\frac{1}{N}\sum_{n=0}^{N-1} m_n^4$) of different modulation formats. For QPSK and 8/16/64QAM signals, the centroid amplitude of m_n^4 is high enough to obtain the peak of its periodogram. However, the centroid amplitude is much lower for 32-QAM signal. As a result, the periodogram peak of m_n^4 is hard to obtain because it is vulnerable to ASE noise.

2.2 Phase Rotation Based Frequency Offset Estimation

Fig. 1 shows that the centroid amplitude of m_n^4 for 32-QAM signal was effected by the distribution of the modulated phase. Considering the effect of the modulated phase, the factor γ is defined as in our previous work [17]:

$$\gamma = \frac{\left|\sum_{n=0}^{N-1} m_n^4\right|}{\sum_{n=0}^{N-1} \left|m_n^4\right|} \times 100\% \tag{3}$$

The factor γ is calculated without taking the addictive white Gaussian noise (AWGN) into account. Using the factor γ, the influence of the modulated phase can be well characterized. If the influence of the modulated phase is completely eliminated after the 4th power operation, γ will take the maximum value as 1. Otherwise, the value of γ is less than 1. In order to increase the value of centroid amplitude for 32-QAM signal, digital amplification and phase rotation are employed in the DSP.

Fig. 2(a) shows the constellation points of 32-QAM signal. Fig. 2(b) shows the points after 4th power operation. It can be seen that the points on each ring are symmetric with respect to the X-axis. The centroid of red points and the centroid of blue points are both on the X-axis and have a π rad phase difference. So the value of factor γ will increase if the points on C2 and C4 rings are rotated by π rad. Meanwhile, considering the C2 ring with less contribution to the centroid

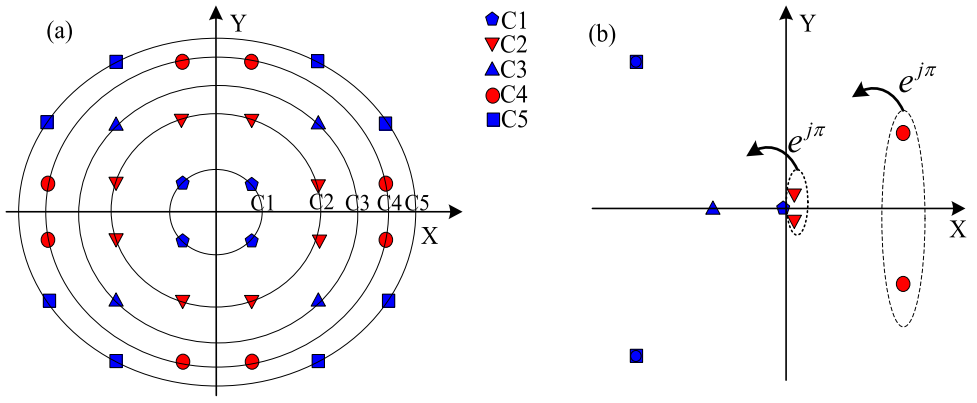

Fig. 2. (a) The constellation of 32-QAM signal and (b) the points of 32-QAM signal after 4th power operation.

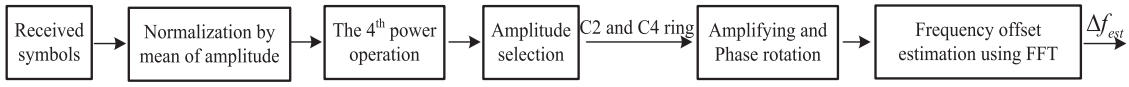

Fig. 3. Block diagram of phase rotation based frequency offset estimation.

TABLE 1
The Value of γ Before and After Rotation

Modulation format	QPSK	8-QAM	16-QAM	32-QAM	64-QAM
Before rotation	100%	87.49%	51.52%	14.50%	44.83%
After rotation	100%	100%	51.52%	70.29%	56.59%

amplitude of m_n^4, the amplitude of C2 ring is digitally amplified up to the same amplitude with the C4 ring.

The block diagram of phase rotation based frequency offset estimation is shown in Fig. 3. Firstly, the received symbols are normalized by mean value of their amplitude. Then, 4th power operation is performed on the normalized samples to obtain constellation points of m_n^4. There are 5 rings with amplitudes of 0.0125, 0.3123, 1.0118, 2.1111, and 3.6101. The C2 ring is digitally amplified up to 2.1111 and then the C2 and C4 rings are digitally rotated by an angle π. Finally, the frequency offset can be obtained by recording the peak location of the periodogram S_n^4.

By amplifying the C2 ring and fixing the rotation angle as $\gamma = 180°$ for C2 and C4 rings, Table 1 shows the value of γ for different modulation formats before and after digital amplification and phase rotation. It can be found that the value of γ after rotation can be kept constant or improved compared to before rotation, especially for 32-QAM signal.

Fig. 4 shows the probability of $|m_n^4|$ for QPSK and 8/16/32QAM signals. The constellation points whose amplitude varies from 0.1 to 0.32 and the constellation points whose amplitude varies from 0.6 to 2.6 will be chosen as rotation region. So the C2 and C4 rings of 32-QAM signal are selected by amplitude after the normalization and 4th power operation. The constellation points of QPSK and 16-QAM signal will not be chosen as rotation region. As a result, the values of γ for QPSK and 16-QAM signals after rotation can be kept constant compared to before rotation. Parts of

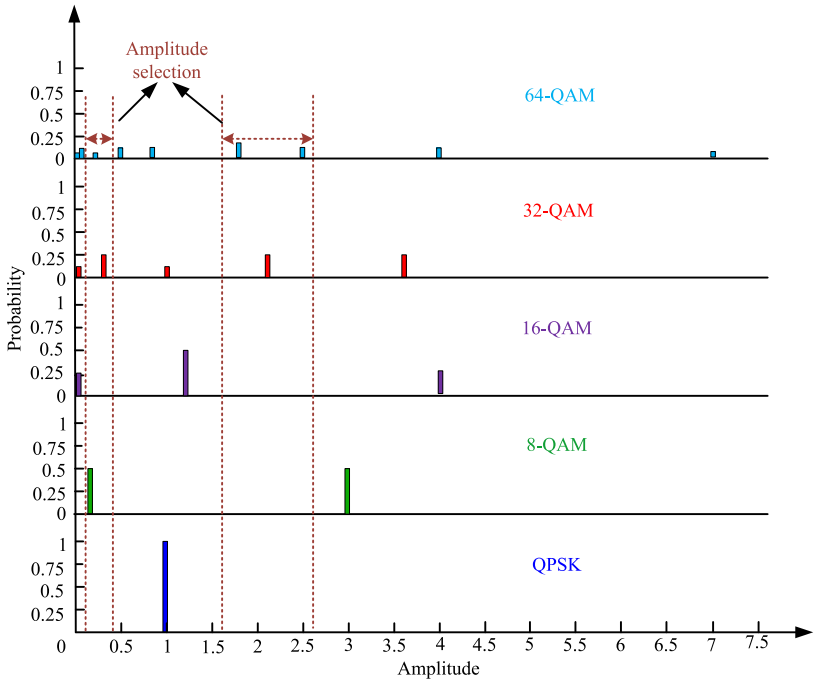

Fig. 4. The probability of $|m_n^4|$ for different modulation formats.

constellation points for 8-QAM and 64-QAM signals will be chosen and rotated. Fortunately, Table 1 shows that the values of γ is improved.

Fig. 5 shows the periodograms of S_n^4 with and without digital amplification and phase rotation for QPSK and 8/16/32/64QAM signals. The length of the FFT is 512. It can be found that the intensity peak becomes obviously for 32-QAM signal with digital amplification and phase rotation. At the same time, the intensity peak can be kept constant or improved for QPSK and 8/16/64QAM signals, which indicates that the proposed algorithm is transparent to QPSK and 8/16/32/64QAM signals. The results indicate that factor γ can theoretically analyze whether the FFT based frequency offset estimation algorithm can be applied. In the process of frequency offset estimation, the proposed amplification and phase rotation method is applied without calculating the factor γ.

3. Simulation Results

The simulation system setup is shown in the Fig. 6. VPI transmission Maker is used to carry out simulations. 28 Gbaud QPSK and 8/16/32/64QAM signals are generated and the linewidth of laser is 100 kHz. The length of pseudo-random bit sequences (PRBS) is $2^{30} - 1$. The OSNR of the optical signal can be controlled by Set OSNR module. At the coherent receiver side, the frequency offset estimation is performed with the proposed method.

The performance of the proposed method for 28 Gbaud 32-QAM signal with different frequency offsets is investigated. The OSNR is set to 22 dB corresponding to SD-FEC threshold [18]. The length of the FFT is 512. Fig. 7(a) shows that the estimated frequency offset is accurate within the range of [−symbol rate/8, +symbol rate/8], i.e., [−3.5 GHz, +3.5 GHz] for 28 Gbaud 32-QAM signals. Fig. 7(b) shows the frequency offset estimation error under various frequency offsets. Due to the limited spectral resolution caused by short block length of 512, the theoretical frequency offset estimation error is in the range of $[-\frac{1}{4\times FFT_{size}\times T_s\times 2}, +\frac{1}{4\times FFT_{size}\times T_s\times 2}]$. Fig. 7(b) indicates that the measuring error with our proposed method is in the theoretical error range.

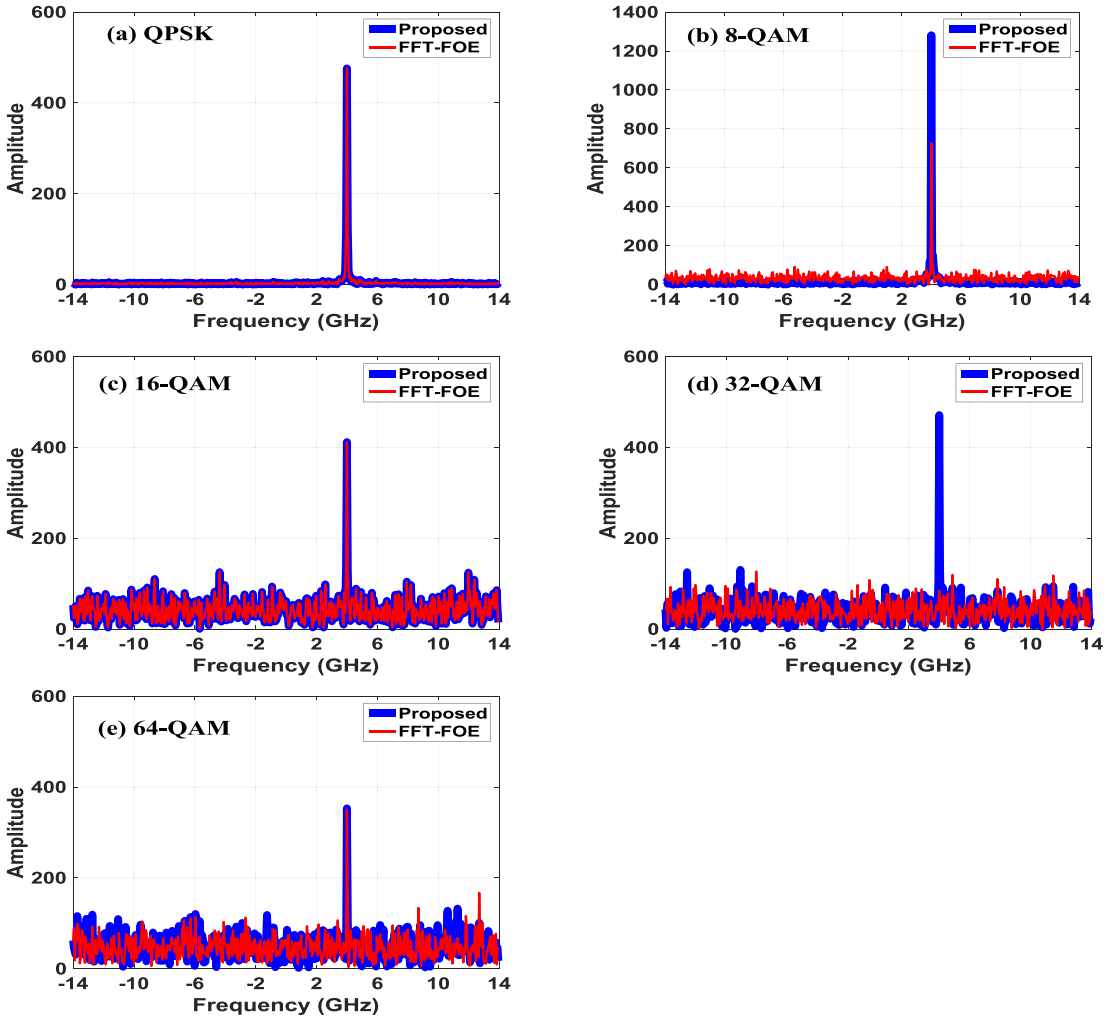

Fig. 5. The periodogram of S_n^4 for 28 Gbaud (a) QPSK, (b) 8-QAM, (c) 16-QAM, (d) 32-QAM, and (e) 64-QAM under the condition of OSNR = 30 dB. The frequency offset is set to 1 GHz and symbol rate is 28 Gbaud.

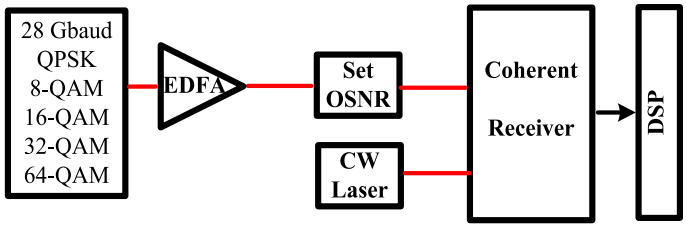

Fig. 6. Simulation system setup. EDFA: Erbium-doped fiber amplifier. CW laser: continuous-wave laser.

Fig. 8 compares the BER for a 28 Gbaud 32-QAM system, and the frequency offset estimation is performed by our proposed method and conventional FFT-FOE method, and 2^{19} samples are used to calculate the BER. The carrier phase recovery uses the blind phase search (BPS) method [19]. For conventional FFT-FOE, due to its severe frequency offset estimation error for 32-QAM, the BER is too high to tolerate even when the FFT size is 1024. Fortunately, with the operation of digital

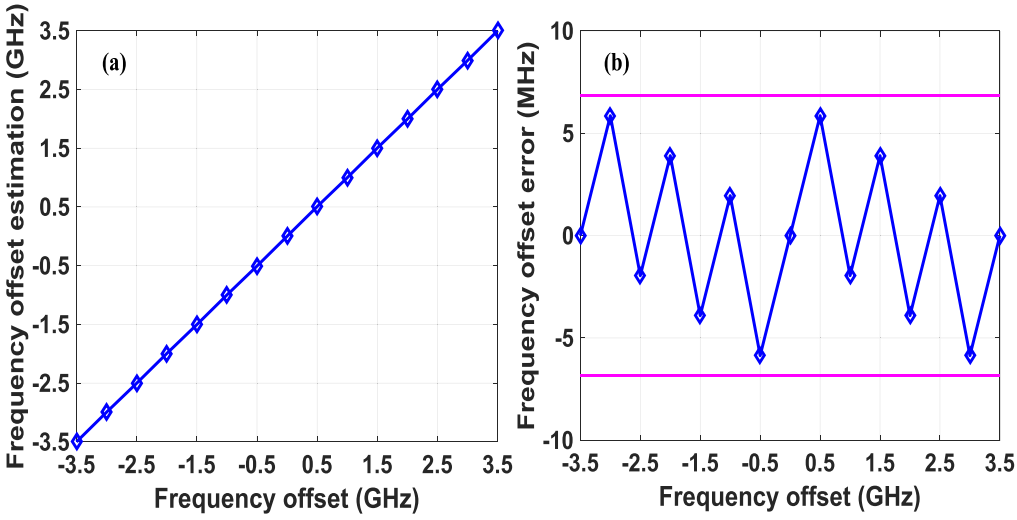

Fig. 7. (a) Performance of the proposed method for 28 Gbaud 32-QAM signal with different frequency offsets and (b) frequency offset estimation error of the proposed method under various frequency offsets.

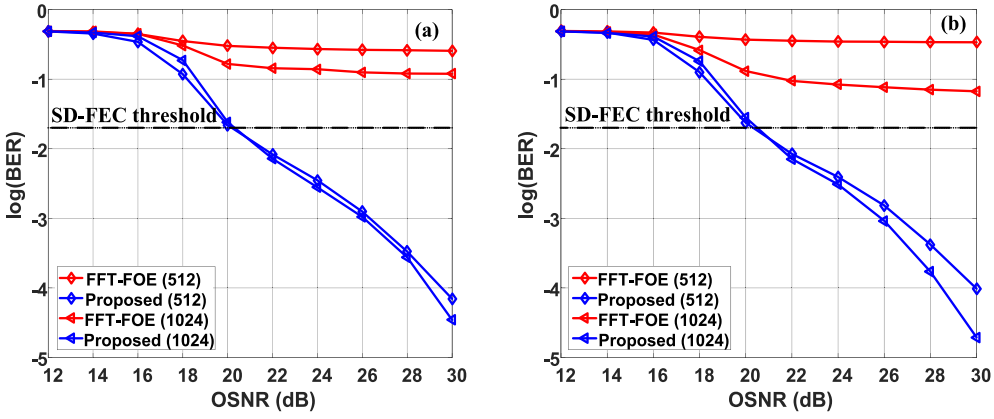

Fig. 8. BER calculation for 28 Gbaud 32-QAM signal with different OSNRs when (a) the frequency offset is 1 GHz and (b) the frequency offset is 3 GHz.

amplification and phase rotation, the 32-QAM signal can be correctly recovered and the BER at OSNR of 22 dB is lower than the SD-FEC threshold with the FFT size of 512. It can be concluded that the digital amplification and phase rotation based FFT-FOE algorithm can realize the frequency offset estimation of 32-QAM signal with OSNR range 22–30 dB using only 512 symbols.

In order to evaluate the robustness to ASE noise of the proposed method, 1000 rounds of the simulation for each condition are performed for observing the normalized mean-square-error (MSE) of the frequency offset estimation, where the normalized MSE is defined as $E[|\Delta f_{est} \cdot T_s - \Delta f \cdot T_s|^2]$. We compare our proposed method with the QPSK-selection assisted FFT-FOE for 28 Gbaud 32-QAM signal [16]. The length of the FFT is 512. The QPSK-selection assisted FFT-FOE selects and digitally amplifies the inner QPSK ring of 32-QAM. The value of γ is 70.29% for our proposed method while the value of γ is 62.71% for QPSK-selection assisted FFT-FOE algorithm. Thus, the periodogram peak can be obtained more easily with the aid of increased γ. The results in Fig. 9 show that the required OSNR of our proposed method is 2 dB lower than QPSK-selection assisted

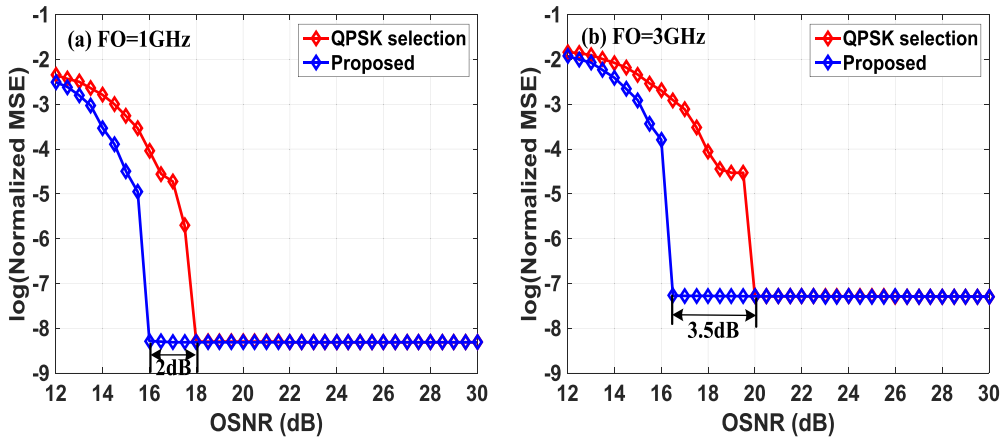

Fig. 9. Comparison of the frequency estimation accuracy for 28 Gbaud 32-QAM signal with our proposed method and the QPSK-selection assisted FFT-FOE when (a) the frequency offset is 1 GHz and (b) the frequency offset is 3 GHz.

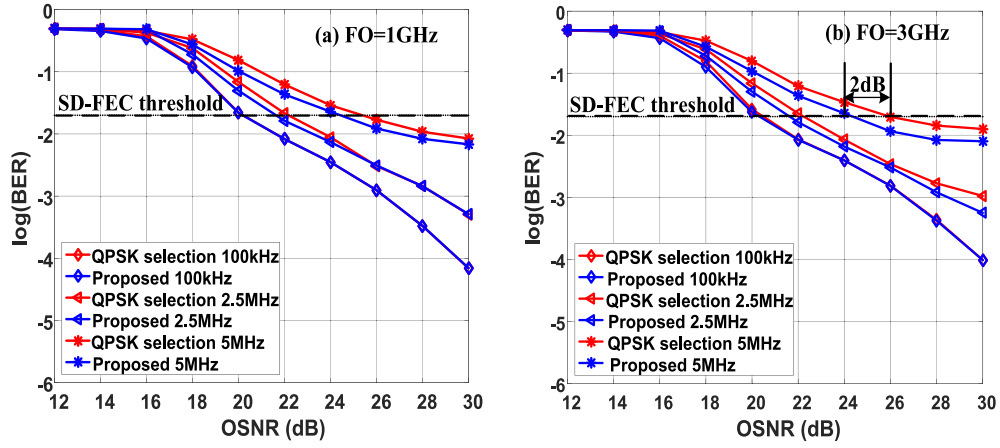

Fig. 10. BER for 28 Gbaud 32-QAM signal with different OSNRs and laser linewidths.

FFT-FOE method and high accuracy of frequency offset estimation can be realized even with low OSNR. The results indicate that the proposed method is more robust to ASE noise.

Fig. 10 shows BER performance with different OSNRs and laser linewidths using our proposed method and QPSK-selection assisted FFT-FOE for 28 Gbaud 32-QAM signal. In Fig. 10(b), if BER at SD-FEC limit is considered, the required OSNR is relaxed by 2 dB when the laser linewidth is greater than 5 MHz, which indicates that the proposed method has better robustness to phase noise. This will make sense when the low-cost laser with wide linewidth is used in short reach optical communication system [20]. Meanwhile, the factor γ can be used for modulation format identification as reported in our previous work [17].

In refs. [13], [15], conventional FFT-FOE can be used for frequency offset estimation for QPSK and 8/16/64QAM signals with 512 symbols. Fig. 5 compares the periodograms of S_n^4 for QPSK and 8/16/64QAM signals with our proposed method and the conventional FFT-FOE, and Table 1 shows that the intensity peak of periodogram can be kept constant or improved for QPSK and 8/16/64QAM signals. Therefore, it is not hard to understand that the proposed algorithm can be also applied for QPSK and 8/16/64QAM signals. Fig. 11 shows the comparison of the proposed method and the conventional FFT-FOE for QPSK and 8/16/64QAM signals. The length of the FFT is 512. It can be

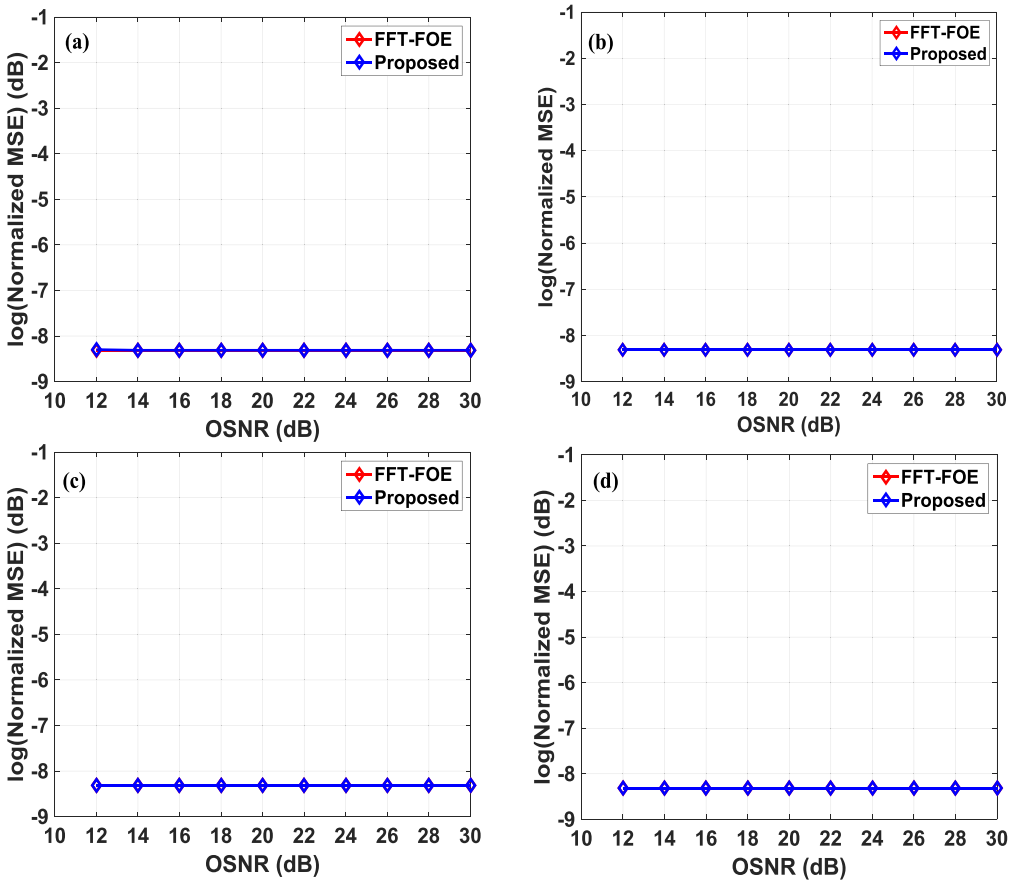

Fig. 11. The comparison of the proposed method and the conventional FFT-FOE for (a) QPSK, (b) 8-QAM, (c) 16-QAM, and (d) 64-QAM signals. (FO = 1 GHz).

seen that the proposed method has the same performance with traditional FFT-FOE even when the OSNR is 12 dB. Therefore, the proposed method can be also applied for QPSK and 8/16/64QAM signals. It should be pointed out here that, the proposed algorithm can be extended to estimate the frequency offset for 128-QAM signal if proper rotation regions are selected.

4. Experimental Results

Next, we conduct 10 Gbaud 32-QAM transmission system, as shown in Fig. 12(a). At the transmitter side, a 100 kHz linewidth continuous-wave (CW) laser with the wavelength of 1550 nm is used. Using an arbitrary waveform generator (AWG) and IQ modulator, the CW laser is modulated as 10 Gbaud 32-QAM signal. The optical signal is then amplified to 0 dBm and launched into an EDFA based fiber recirculating loop. An optical attenuator is placed after EDFA to adjust OSNR. The OSNR of optical signal can be monitored using optical spectrum analyzer (OSA). At the receiver side, another CW laser with 100 kHz linewidth is used to set frequency offset and the signal is digitized by 50 GSa/s real-time scope after coherent detection. Fig. 12(b) shows the frame structure in the experiment which consists of 16384 QPSK symbols and 16384 32-QAM data sequence. Similar to [15], the 16384 QPSK symbols are used to calculate the frequency offset using traditional FFT-FOE as the evaluation criterion.

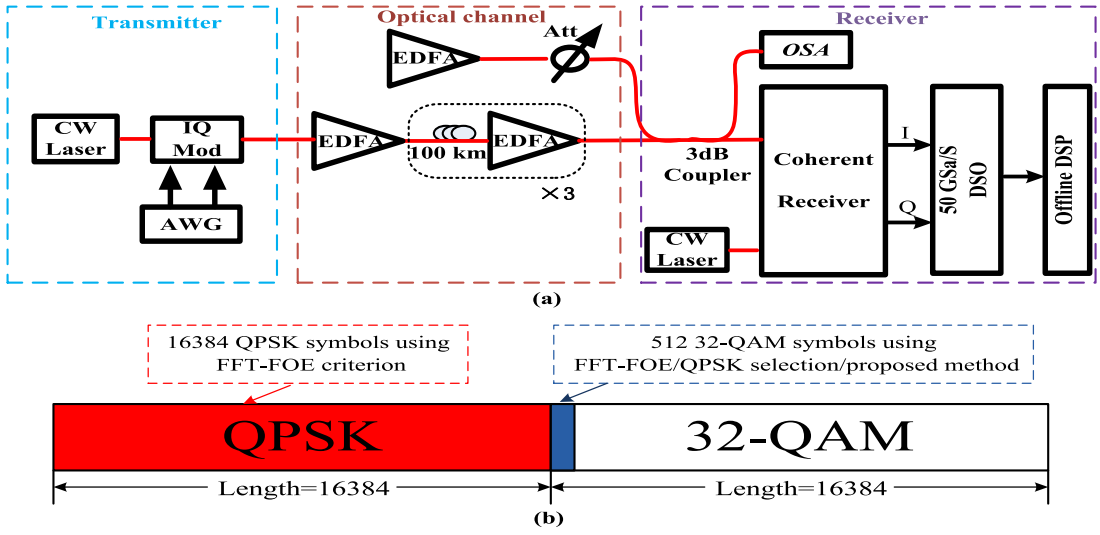

Fig. 12. (a) Experimental setup for 10 Gbaud 32-QAM system. ATT: attenuator. (b) Frame structure.

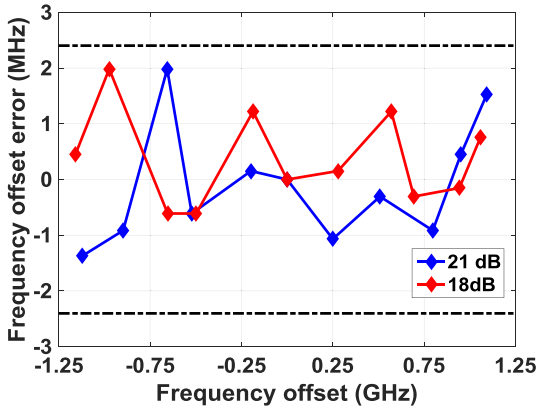

Fig. 13. Frequency offset estimation error of the proposed method d for 10 Gbaud 32-QAM signal under various frequency offsets.

Fig. 13 shows the frequency offset estimation error under various frequency offsets. Please note that the frequency offset evaluation criterion using 16384 QPSK symbols also has limited spectral resolution. So the theoretical frequency offset estimation error is in the range of $[-\frac{1}{4\times FFT_{size}\times T_s\times 2}+\frac{1}{4\times 16384\times T_s\times 2}, \frac{1}{4\times FFT_{size}\times T_s\times 2}-\frac{1}{4\times 16384\times T_s\times 2}]$. Fig. 13 indicates that the measuring error with our proposed method is in the theoretical error range.

We start to experimentally evaluate performance for B2B system. 32 data sets at each OSNR are collected to evaluate the normalized MSE. Fig. 14 shows that comparison with three different frequency offset estimation methods. The FFT size is 512 symbols. Based on the theoretical frequency offset error range, the theoretical normalized MSE threshold is proposed. It shows that the digital amplification and phase rotation based FFT-FOE algorithm can realize the frequency offset estimation of 32-QAM signal when OSNR is greater than 14 dB. The required OSNR of our proposed method is 2 dB lower than QPSK-selection assisted FFT-FOE method.

To further verify the feasibility of proposed method, we test long-haul transmission performance. We use the overlap frequency domain equalization (OFDE) algorithm to compensate CD. The frequency offset is 1 GHz. Fig. 15 shows that the proposed method can be applied in optical

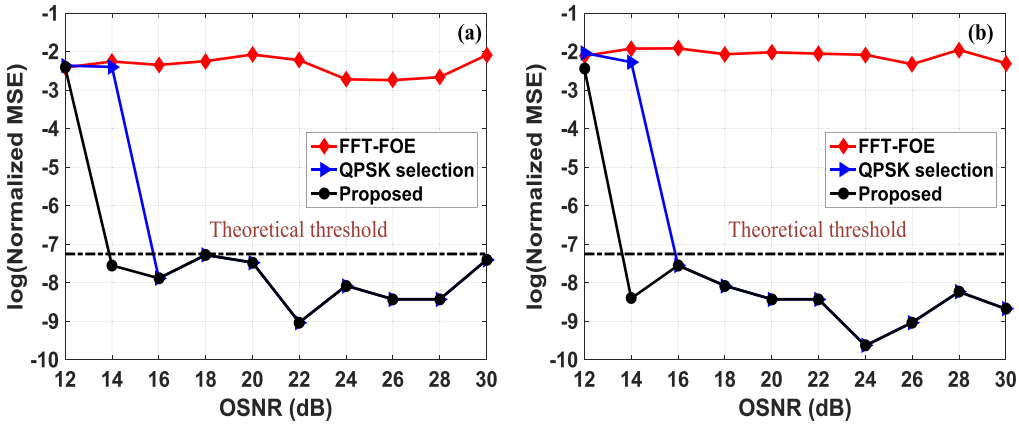

Fig. 14. The normalized MSE for 10 Gbaud 32-QAM signal as a function of OSNR, (a) FO = 0.5 GHz, (b) FO = 1 GHz.

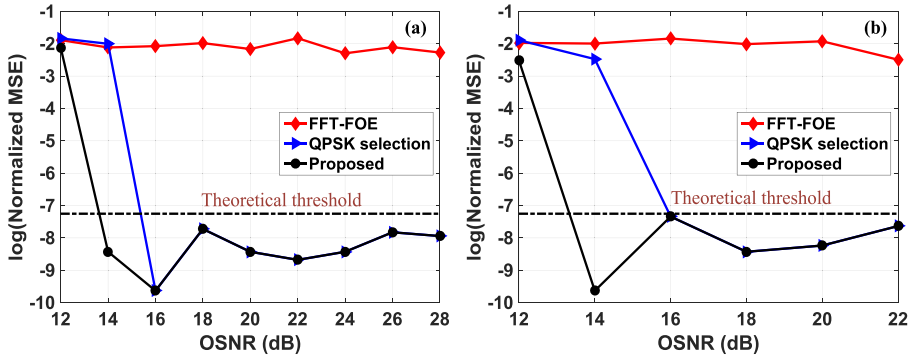

Fig. 15. The normalized MSE for 10 Gbaud 32-QAM signal with transmission of (a) 100 km and (b) 300 km.

fiber communication systems and has better performance than QPSK-selection assisted FFT-FOE method.

5. Computation Complexity Analysis

In practical applications, the complexity of DSP algorithm is critical. For QPSK-selection assisted FFT-FOE method, it takes $2N\log 2N + 14N + 2$ real multipliers, $3N\log N + 6N$ real adders and $2N$ comparators for a FFT size of N symbols [16]. For our proposed method, it takes $2N\log 2N + 15N + 2$ real multipliers, $3N\log N + 6N$ real adders and $3N$ comparators for a FFT size of N symbols. Two methods have the same FFT size as 512. The complexity of proposed method is slightly higher than QPSK-selection assisted FFT-FOE method. Therefore, the complexity of proposed method is acceptable.

6. Conclusions

In this paper, we propose a blind FFT-FOE algorithm for coherent transceiver, which is transparent to QPSK and 8/16/32/64QAM signals. A factor γ is proposed to determine whether the FFT based algorithm can be used for frequency offset estimation. By performing amplification and phase rotation on part of the 4^{th} power constellation points, the value of γ is increased and the FFT

based algorithm can be used to estimate the frequency offset. The results on 28 Gbaud 32-QAM system demonstrate that the proposed method has higher frequency offset estimation accuracy and the required OSNR is 2 dB lower than that of QPSK-selection assisted FFT-FOE method. The BER of 28 Gbaud 32-QAM signal with OSNR of 22 dB is lower than that of SD-FEC limit. We also investigate the tolerance to phase noise. The results demonstrate that, with the proposed method, the required OSNR is relaxed by 2 dB when the low-cost laser with linewidth greater than 5 MHz is considered, which is used in short reach optical fiber communication systems. The experimental results by B2B and 300 km fiber transmission system using 10 Gbaud 32-QAM signal shows that our proposed method can be applied when OSNR is greater than 14 dB and has better performance than QPSK-selection assisted FFT-FOE method. Furthermore, the proposed method can also be applied to QPSK and 8/16/64QAM system, which is preferred by a coherent receiver.

References

[1] K. Roberts and C. Laperle, "Flexible transceivers," in *Proc. Eur. Conf. Exhib. Opt. Commun.*, 2012, pp. 1–3.
[2] M. T. Nag, and B. Mukherjee, "Optical network design with mixed line rates and multiple modulation formats," *IEEE J. Lightw. Technol.*, vol. 28, no. 4, pp. 466–475, Feb. 2010.
[3] T. Teipen, M. H. Eiselt, K. Grobe, and J.-P. Elbers, "Adaptive data rates for flexible transceivers in optical networks," *IEEE J. Netw.*, vol. 7, no. 5, pp. 776–782, May 2012.
[4] P. Isautier, J. Pan, R. DeSalvo, and S. Ralph, "Stokes space-based modulation format recognition for autonomous optical receivers," *IEEE J. Lightw. Technol.*, vol. 33, no. 24, pp. 5157–5163, Dec. 2015.
[5] F. N. Khan *et al.*, "Modulation format identification in coherent receivers using deep machine learning," *IEEE Photon. Technol. Lett.*, vol. 28, no. 17, pp. 1886–1889, Sep. 2016.
[6] F. N. Khan *et al.*, "Joint OSNR monitoring and modulation format identification in digital coherent receivers using deep neural networks," *Opt. Express*, vol. 25, no. 15, pp. 17767–17776, 2017.
[7] A. Meiyappan, P. Kam, and H. Kim, "On decision aided carrier phase and frequency offset estimation in coherent optical receivers," *IEEE J. Lightw. Technol.*, vol. 31, no. 13, pp. 2055–2069, Jul. 2013.
[8] J. Lu *et al.*, "Joint carrier phase and frequency-offset estimation with parallel implementation for dual-polarization coherent receiver," *Opt. Express*, vol. 25, no. 5, pp. 5217–5231, 2017.
[9] A. Leven, N. Kaneda, U. V. Koc, and Y. K. Chen, "Frequency estimation in intradyne reception," *IEEE Photon. Technol. Lett.*, vol. 19, no. 6, pp. 366–368, Mar. 2007.
[10] I. Fatadin and S. J. Savory, "Compensation of frequency offset for 16-QAM optical coherent systems using QPSK partitioning," *IEEE Photon. Technol. Lett.*, vol. 23, no. 17, pp. 1246–1248, Sep. 2011.
[11] J. Lu *et al.*, "Frequency offset estimation for 32-QAM based on constellation rotation," *IEEE Photon. Technol. Lett.*, vol. 29, no. 23, pp. 2115–2118, Dec. 2017.
[12] T. Yang *et al.*, "Hardware-efficient multi-format frequency offset estimation for M-QAM coherent optical receivers," *IEEE Photon. Technol. Lett.*, vol. 30, no. 18, pp. 1605–1608, Sep. 2018.
[13] M. Selmi, Y. Jaouen, and P. Ciblat, "Accurate digital frequency offset estimator for coherent polmux QAM transmission system," in *Proc. Eur. Conf. Exhib. Opt.Commun.*, 2009, pp. 1–2.
[14] G. Liu, R. Proietti, K. Zhang, H. Lu, and S. J. Ben Yoo, "Blind modulation format identification using nonlinear power transformation," *Opt. Express*, vol. 25, no. 25, pp. 30895–30904, 2017.
[15] S. Fu *et al.*, "Modulation format identification enabled by the digital frequency-offset loading technique for hitless coherent transceiver," *Opt. Express*, vol. 26, no. 6, pp. 7288–7296, 2018.
[16] F. Xiao *et al.*, "Feed-forward frequency offset estimation for 32-QAM optical coherent detection," *Opt. Express*, vol. 25, no. 8, pp. 8828–8839, 2017.
[17] Q. Tan, A. Yang, and P. Guo, "Blind modulation format identification using the DC component," *IEEE Photon. J.*, vol. 11, no. 2, Apr. 2019, Art. no. 7902910.
[18] X. Mai *et al.*, "Stokes space modulation format classification based on non-iterative clustering algorithm for coherent optical receivers," *Opt. Express*, vol. 25, no. 3, pp. 2038–2050, 2017.
[19] T. Pfau, S. Hoffmann, and R. Noé, "Hardware-efficient coherent digital receiver concept with feedforward carrier recovery for M-QAM constellations," *IEEE J. Lightw. Technol.*, vol. 27, no. 8, pp. 989–999, Apr. 2009.
[20] X. Xue *et al.*, "Wide-linewidth coherent systems with parallelized extended Kalman filter for data center interconnection," *Opt. Commun.*, vol. 458, pp. 124740–124740, 2020.